Climatic Change (2011) 109 (Suppl 1):S445–S463
DOI 10.1007/s10584-011-0329-9

Climate change and growth scenarios for California wildfire

A. L. Westerling · B. P. Bryant · H. K. Preisler · T. P. Holmes · H. G. Hidalgo · T. Das · S. R. Shrestha

Received: 21 September 2011 / Accepted: 17 October 2011 / Published online: 24 November 2011

Abstract Large wildfire occurrence and burned area are modeled using hydroclimate and landsurface characteristics under a range of future climate and development scenarios. The range of uncertainty for future wildfire regimes is analyzed over two emissions pathways (the Special Report on Emissions Scenarios [SRES] A2 and B1 scenarios); three global climate models (Centre National de Recherches Météorologiques CM3, Geophysical Fluid Dynamics Laboratory CM2.1 and National Center for Atmospheric Research PCM1); three scenarios for future population growth and development footprint; and two thresholds for defining the wildland-urban interface relative to housing density. Results were assessed for three 30-year time periods centered on 2020, 2050, and 2085, relative to a 30-year reference period centered on 1975. Increases in wildfire burned area are anticipated for most scenarios, although the range of outcomes is large and increases with time. The increase in wildfire burned area associated with the higher emissions pathway (SRES A2) is substantial, with increases statewide ranging from 36% to 74% by 2085, and increases exceeding 100% in much of the forested areas of Northern California in every SRES A2 scenario by 2085.

Electronic supplementary material The online version of this article (doi:10.1007/s10584-011-0329-9) contains supplementary material, which is available to authorized users.

A. L. Westerling (✉) · S. R. Shrestha
University of California, Merced, 5200 N. Lake Rd, Merced, CA 95343, USA
e-mail: awesterling@ucmerced.edu

B. P. Bryant
Pardee RAND Graduate School, The RAND Corporation, Santa Monica, CA, USA

H. K. Preisler
USDA Forest Service Pacific Southwest Research Station, Albany, CA, USA

T. P. Holmes
USDA Forest Service Southern Research Station, Research Triangle Park, NC, USA

H. G. Hidalgo
School of Physics and Center for Geophysical Research, University of Costa Rica, San Jose, Costa Rica

T. Das
CH2MHILL, Inc., San Diego, CA 92101, USA

1 Introduction

The climate system interacts with various factors such as soils, topography, available plant species, and sources of ignition to give rise to both natural ecosystems and their fire regimes. Long-term patterns of temperature and precipitation determine the moisture available to grow the vegetation that fuels wildfires (Stephenson 1998). Climatic variability on interannual and shorter scales governs the flammability of these fuels (e.g., Westerling et al. 2003; Heyerdahl et al. 2001; Kipfmueller and Swetnam 2000; Veblen et al. 2000; Swetnam and Betancourt 1998; Balling et al. 1992). Flammability and fire frequency in turn affect the amount and continuity of available fuels. Consequently, long-term trends in climate can have profound implications for the location, frequency, extent, and severity of wildfires and for the character of the ecosystems that support them (Westerling 2009).

Human-induced climatic change may, over a relatively short time period (< 100 years), give rise to climates outside anything experienced in California since the establishment of an industrial civilization currently sustaining a state population that has increased approximately 41,000% since 1850. Changes in wildfire regimes driven by climate change are likely to impact ecosystem services that California citizens rely on, including carbon sequestration in California forests; quality, quantity and timing of water runoff; air quality; wildlife habitat; viewsheds and recreational opportunities. They may also impact the ability of homeowners and federal, state, and local authorities to secure homes in the wildland-urban interface from damage by wildfires (Westerling and Bryant 2008).

In addition to climate change, the continued growth of California's population and the spatial pattern of development that accompanies that growth are likely to directly affect wildfire regimes through their effects on the availability and continuity of fuels and the availability of ignitions. They are also likely to impact both wildfire and property losses due to wildfire through their effects on the extent and value of development in California's wildland-urban interface, both through their effects on the number of structures proximate to wildfire risks and their effects on fire suppression strategies and effectiveness.

The combined effects of climate change and development on California's future large wildfire occurrence and burned area are the focus of the research presented here. Our modeling projects California's fire regimes as they are currently managed onto scenarios for future climate, population, and development. The methodology we employ can incorporate the effects of spatial variations in current management strategies on average fire risks. However, the monthly and interannual variations in large wildfire occurrence and burned area that we estimate do not reflect changes in management strategies over time, although our modeling does have the capacity to reflect changes in the effectiveness of current management strategies to the extent that these changes currently tend to correlate with climate and landsurface characteristics. Thus, hypothetical effects of future changes in management in response to the impacts of climate and development on wildfire are not considered in this work.

The metrics we model—large fire occurrence and burned area—are not the only metrics we would wish to employ to assess the full range of the ecological and human impacts of wildfire. In particular, metrics of fire severity (e.g., the percent of available biomass consumed, characteristics of ecological impacts) would be highly desirable as well. These metrics are likely to change in response to climate, may also be influenced by future management decisions, and are key components for estimating many wildfire impacts due to climate change. The work reported here does not consider changes in fire severity, which are the target of multiple ongoing research efforts. However, in interpreting our results, it would be a mistake to assume a linear correspondence between increased burned area and fire severity. Fire severity is likely to increase in some ecosystems and decrease in others alongside increases in burned area.

Furthermore, severity might decrease in some ecosystems for reasons that many California residents would find undesirable (i.e., broad-scale changes in ecosystems).

This work extends an analysis by Westerling and Bryant (2008) that considered the effects of climate change on California large (>200 ha) wildfire occurrence and wildfire-related damages holding development fixed at the 2000 census. In this analysis we statistically model large (>200 and >8,500 ha) wildfire occurrence as a product of both future climate scenarios and future population and development scenarios, using nonlinear logistic regression techniques developed for seasonal wildfire forecasting in California and the western United States (Preisler and Westerling 2007). We model the expected burned area using Generalized Pareto Distributions fit to observed wildfires >200 and >8,500 ha. We assess a range of outcomes given numerous sources of uncertainty, including three global climate models (GCMs) with different sensitivities of temperature and precipitation to anthropogenic forcing, two emissions scenarios, and three population growth and development scenarios. Our goal is not to determine one most likely outcome, but rather to define a population of plausible outcomes, which can then be used in future work to assess the robustness of combined adaptation and mitigation policy choices.

2 Data and methods

2.1 Domain and resolution

The spatial domain for this analysis was a 1/8-degree lat/long grid (~12 km resolution) bounded by the political boundary for the state of California. Areas of the state outside the current combined fire protection responsibility areas of the California Department of Forestry and Fire Protection and contract counties (combined here and denoted CDF), the U.S. Department of Agriculture's Forest Service (USFS), and the U.S. Department of Interior's National Park Service (NPS), Bureau of Land Management (BLM), and Bureau of Indian Affairs (BIA) were excluded. The result was a set of 2,267 grid cells within the State. Fire was then modeled over this domain at monthly time-steps for historic and simulated climate scenarios.

Five time periods were used for this analysis. Coefficients for statistical wildfire models were estimated using monthly, gridded, historical fire and climate data available for 1980–1999. These coefficients were then applied to gridded climate scenarios derived from GCMs, and the results for three future climate periods—2005–2034, 2035–2064, and 2070–2099 (henceforth referred to as 2020, 2050, and 2085) were compared to a common reference period (1961–1990, henceforth 1975) for each scenario. These comparisons used average annual fire occurrence and burned area statistics computed for each 30-year period referenced above.

2.2 Fire history

A comprehensive wildfire history for California for 1980–1999[1] was assembled from digital fire records obtained from CDF, USFS, NPS, BLM, and BIA. The CDF records included perimeters for large fires under both direct CDF and contract counties' fire protection responsibility (obtained online at http://frap.cdf.ca.gov/). Federal fires were

[1] Comprehensive data prior to 1980 are not available from some of these sources. Fire data after 1999 are available, but the hydrologic simulations forced with historic climate data used here were developed for the California Scenarios Project, of which this research is a component. These data ended in 1999, so the common period of overlap between the available fire history and the hydroclimatic data was 1980–1999.

sourced from point data records compiled from individual fire reports. The methods used in compiling these data are described in Westerling et al. (2006, online supplement) and Westerling and Bryant (2008). Westerling et al. (2002) describe in detail the federal data in this sample and their response to climate variability.

Our wildfire history was aggregated to a 1/8-degree gridded monthly data set of frequencies of fires >200 ha in burned area and the total burned area in these large wildfires (544,080 data points=2,267 grid points × 20 years × 12 months/year). Wherever we refer to fire occurrence in the text, we are referring to the occurrence of wildfires greater than 200 ha, unless otherwise specified. For federal-sourced wildfire data, fires were allocated to the grid cell in which they were reported to have ignited. For CDF fires reported as polygon perimeters, fires were allocated to the grid cell corresponding to their centroid. Fires were assigned to the month in which they were discovered. In many cases fires continued to burn for additional months, but we did not have the means to apportion burned area by month.

Wildfires managed by the Fisheries and Wildlife Service (FWS), the Department of Defense (DOD), and the Bureau of Reclamation (BOR) were not included because they were not available with sufficient comprehensiveness and quality. The FWS and BOR lands are relatively small in area and—particularly in the case of FWS—located in areas (e.g., California's Central Valley) that would likely have been excluded from this analysis for other reasons. The Department of Defense lands in California are significant, similar in scale to those of NPS. We could extend our analysis spatially to DOD lands by applying model coefficients estimated using other agencies' fire histories to DOD lands, for which we have the explanatory variables. However, the vast majority of DOD lands in California lie in southeastern desert areas of the state, which show negligible changes in fire risks by the end of the twenty-first century under many, though not all, of our scenarios.

2.3 Land surface characteristics

2.3.1 Vegetation

Coarse vegetation characteristics used here were compiled from the Land Data Assimilation System (LDAS) for North America's 1/8-degree gridded vegetation layers that use the University of Maryland vegetation classification scheme with fractional vegetation adjustment (UMDvf) (Mitchell et al. 2004; Hansen et al. 2000) (For an analysis of how our modeling relates to the LDAS vegetation categories, see the supplemental materials.)

In our modeling, the primary variable we use from LDAS is the fraction of each grid cell that is vegetated and not used for agriculture (V). In our model for estimating fire probabilities, V plays an important role. In the limit of complete urbanization, it is clear that this variable is affected by encroaching human development, because a grid cell entirely covered by dense population would lack any sufficiently large vegetated space in which wildfires could exist. However, vegetation cover may be reduced by encroaching human development at intermediate scales as well, depending on how new growth is allocated. In Section 2.4 and the supplemental materials we describe how scenarios for allocating projected growth within a grid cell affect the vegetation fraction.

2.3.2 Topography

Topographic data on a 1/8-degree grid were also obtained from LDAS. The LDAS topographic layers are derived from the GTOPO30 Global 30 Arc Second (~1 km) Elevation Data Set (Mitchell et al. 2004; Gesch and Larson 1996; Verdin and Greenlee

1996). We tested mean and standard deviation of elevation, slope, and aspect as explanatory variables in our wildfire model specification.

2.3.3 Protection responsibility

Logistic regression techniques attempt to estimate probabilities of wildfires occurring at a given time and location as a function of predictor variables. The predictand is always valued zero or one, and in this case most data points are zero, since fires are relatively rare occurrences at ~12 km × monthly scales. It is important to distinguish between data points that are zero because no fire occurred, and data points that are zero because the fires that may have occurred there are not reported by the agencies included in our sample. The practical effect of including in our modeling areas for which we do not have good fire reports is to underestimate the probability of fire occurrence everywhere on average. We used the fraction of each grid cell's area covered by the protection responsibility of the agencies in our sample to estimate the area over which fires could occur.

A GIS layer of Local, State, and Federal protection responsibility areas in California was obtained online from the CDF Fire and Resource Assessment Program (http://frap.cdf.ca.gov/). The polygons in this layer were extracted and intersected with our 1/8-degree grid to obtain the fraction of each grid cell in Local (LRA), State (SRA), and Federal (FRA) protection responsibility areas. Since federal protection responsibility includes agencies excluded from our sample, we obtained GIS layers of federal and Indian lands online from the United States National Atlas (http://nationalatlas.gov/). These were also extracted and intersected with our grid in order to determine what fraction of the federal responsibility area in each grid cell corresponded to the federal agencies in our sample.

Our analysis was limited to the SRA (for which we have CDF wildfire histories) and those parts of the FRA administered by the federal agencies for which we have wildfire histories (USFS, NPS, BLM, BIA). The LRA was excluded both because we do not have wildfire histories for those lands and because they are predominately developed for urban and agricultural uses. We limited our analysis to grid cells with a combined protection responsibility (SRA, USFS, NPS, BLM, BIA) exceeding 15% of the total grid cell area.

2.4 Growth and development scenarios

We employed spatially explicit 100 m-resolution twenty-first century population growth and development scenarios based on work by Theobald (2005) and developed by the U.S. EPA (2008) as the Integrated Climate and Land Use Scenarios (ICLUS) for the United States. These scenarios incorporate assumptions about future trajectories with regards to sprawl as well as population growth rates based on the Intergovernmental Panel on Climate Change (IPCC) Special Report on Emissions Scenarios (SRES) social, economic, and demographic storylines, downscaled to the United States. We report results here for ICLUS scenarios with growth and sprawl that would be consistent with the global A1 and B2 SRES scenarios, and an intermediate base case trajectory (Table 1). While we do not model spatial variation in wildfire below the 1/8-degree grid threshold, we do consider effects of assumptions about the allocation of new development below that level (see supplemental materials). Our scenarios for allocating development consider the effects of expanding the wildland-urban interface into areas that are currently vegetated versus siting new development in areas that are currently bare or agricultural land. For the intermediate case, we allocate new development proportionately across baseline vegetated, bare and agricultural areas. For the high growth and sprawl scenario (A2), we allocate new

Table 1 ICLUS growth and development scenarios for California

Scenario	2100 CA Population	Change vs 2000	Description (identifier)
A2	81 million	+154%	high growth & sprawl (HIH,HIH)
Base Case	62 million	+84%	medium growth & sprawl (MID,MID)
B1	50 million	+54%	Low growth & sprawl (LOW,LOW)

development to vegetated areas, and for the low growth and sprawl scenario (B1) we allocate new development within bare and agricultural areas. Additionally, we use two different thresholds for describing when a 100 m pixel is fully "urbanized," such that a wildfire cannot occur there: 147 and 1000 households per square kilometer (the limits used in the ICLUS scenarios to define suburban areas).

2.5 Climate and hydrologic data

2.5.1 Historical data

A common set of gridded historical (1950–1999) climate data including maximum and minimum temperature, precipitation (PCP), radiation, and wind were designated for the Second California Assessment (see Maurer et al. 2002; Hamlet and Lettenmaier 2005). We used these data with LDAS vegetation and topography to drive the Variable Infiltration Capacity (VIC) hydrologic model at a daily time step in full energy mode, generating a full suite of gridded hydroclimatic variables such as actual evapotranspiration (AET), soil moisture, relative humidity (RH), surface temperature (TMP) and snow-water equivalent (SWE) (Liang et al. 1994). Because Potential Evapotranspiration (PET) was not easily extracted from the version of the VIC model used here, we used the Penman-Monteith equation to estimate PET directly (Penman 1948; Monteith 1965). Moisture deficit (D) was then calculated from PET and AET (D = PET - AET).

As indicators of drought stress, we calculated the cumulative water-year moisture deficit for each of the preceding 2 years (D01 and D02). Water year (October - September), rather than calendar year, moisture deficit is used because in California most of the precipitation that affects fuel availability and flammability falls between October and April. We also calculated the standardized cumulative moisture deficit from October 1 through the current month (CD0). The 30-year means for 1961–1990 for moisture deficit (D30), AET (AET30), PCP (PCP30), and TMP (TMP30) were also used below to analyze the spatial distribution of climate-vegetation-wildfire interactions to be represented in the wildfire model specification (Electronic Supplementary Material).

2.5.2 Climate scenarios

As described by Cayan et al. (2009), several GCMs and emissions scenarios were selected for the Second California Assessment. In this report we describe results across three models —CNRM CM3, GFDL CM2.1, NCAR PCM—and two emissions scenarios—SRES A2 (a medium-high emissions trajectory) and SRES B1 (a low emissions trajectory) comprising six realizations for future climate. Daily climate data from these models were downscaled to the 1/8-degree grid using the Constructed Analogues method (see Hidalgo et al. 2008; Maurer and Hidalgo 2008). After downscaling, the VIC model was used to simulate the same suite of

hydrologic variables for each target time period (1975, 2020, 2050, 2085) in each climate scenario as described for the historical period (Section 2.5).

As described in Cayan et al. (2009), the models were selected for their fidelity in representing historical California temperature and precipitation in particular, with appropriate seasonality. Also, the selected models were required to simulate tropical Pacific sea surface temperature variability consistent with observed ENSO variability, and to have appropriate spatial resolution over California for the downscaling methodologies employed here. That left a set of six models. Daily precipitation and daily maximum and minimum temperature had to be included in the models' historical and projection saved sets in order to use the Constructed Analogs downscaling methodology, which narrowed the set to three models.

While we only use the three models downscaled with the Constructed Analogs methodology, the larger set of six models show a consensus toward drier conditions in southern and central California, but more scattered results in the region from Lake Shasta to the northernmost parts of California. An unpublished review of a larger set of 12 models showed similar results, increasing our confidence that the models used here are representative of what a larger set of models project for California. So while it is true that our models do not encompass the full range of model uncertainty of the AR4, the GCMs used here appear to cover a range of projected temperature and precipitation that is representative of the state of the art modeling guidance for California. A possibly more relevant concern is that the estimated emissions growth for 2000–2007 exceeded the most fossil fuel-intensive scenario of Intergovernmental Panel on Climate Change (Le Quéré et al 2009). The longer this trend in emissions growth rates persists, the harder it may be to reach a future scenario like those modeled here, and the more likely it is our results may underestimate future impacts.

Each of the GCMs evidences different sensitivities to anthropogenic forcing, with the CNRM CM3 and GFDL CM2.1 models generally showing warmer temperatures than the NCAR PCM, particularly in summer. The other three models assessed by Cayan et al (2009) that are not used here were also warmer than the NCAR PCM. The GFDL CM2.1 model tended to be drier than the others in both northern and southern California in most scenarios, while CNRM CM3 was typically drier than NCAR PCM. Compared to the larger set of models, NCAR PCM is also the least dry by the end of the century under the A2 scenario (Cayan et al 2009). It is not clear how significant variation in precipitation across the models is, since that variation is small compared to the potential natural variability in precipitation in the region. Notably, the tendency towards dryness across all the models is much more pronounced and uniform for California in the A2 emissions scenarios, when anthropogenic forcing is higher, than for the B1 scenarios, and it seems reasonable to speculate that the forcing is overwhelming the natural variation in the A2 scenarios.

The six climate scenarios used here encompass three separate sources of uncertainty for our modeling: the degree of anthropogenic forcing (represented by the A2 and B1 emissions paths), the extent of climate system sensitivity to anthropogenic forcing (greater in GFDL CM2.1 and CNRM CM3 than NCAR PCM), and the range of random variation in climate across 30-year windows in six scenarios (unknowable for a sample of this size).

3 Modeling

3.1 Fire modeling

Because large wildfires are relatively rare events, statistical models for wildfire must aggregate fire occurrence over space and/or time in order to avoid fitting a model of zeros.

Logistic regressions allow us to model wildfire occurrence at arbitrarily fine spatial and temporal resolutions (limited only by the available data) while statistically aggregating across locations with similar characteristics. We estimated the monthly probability of large (>200 ha and >8500 ha) wildfires occurring as a function of land-surface characteristics, human population, and climate on a 1/8-degree grid using generalized linear models in R. Candidate model specifications were tested by comparing the Akaike Information Criterion (AIC) estimated for each model. The best model specification was then tested using leave-one-out cross-validation. That is, for each of the 20 years in the model estimation period, a separate set of model coefficients were estimated using the other 19 years of data.

The climatic variables used here as predictors for fire occurrence (Table 2) were selected to describe variation in moisture available for the growth and wetting of fuels over a range of time scales, from long term averages over 30 years (D30, AET30), to interannual variations in the 3 years through the current year (D01, D02), to seasonal variations and conditions at the month a fire could potentially burn (CD0, PCP, RH, TMP). Westerling and Bryant (2008) and Westerling (2009) show that long-term climate averages can serve as a proxy for coarse vegetation and fire regime types, distinguishing between diverse fire regime responses to antecedent and concurrent climate. Preisler et al (2011), Westerling (2009) and Westerling et al. (2006) show that cumulative annual moisture deficits in the current and 1–2 preceding years are strongly associated with variability in large wildfire occurrence, and the latter work also links large wildfire occurrence to temperature and variations in spring snowmelt timing. Finally, relative humidity (RH) is a key component of many fire weather indices, and a good predictor of fuel moisture (e.g., Schlobohm and Brain 2002).

Vegetation fraction and population are indicators of burnable area, availability of human-origin ignitions, and accessibility. Other variables we tested—such as total protection responsibility area, and mean and standard deviation of elevation—were not included in the model specification because they did not substantially improve model fit as measured by the AIC. The climatic and land surface variables we selected are not independent of topography and protection responsibility area. Federal protection responsibility and U.S. Forest Service protection responsibility area were highly significant, and may be indicative of differences in management or resources across protected areas, or they may be proxies for other spatial variables such as accessibility, vegetation type, sources of ignitions, etc.

The model specification employed here for estimating fire occurrence builds on Preisler and Westerling (2007) and Westerling and Bryant (2008), and adopts methodologies presented in Brillinger et al. (2003), and Preisler et al. (2004):

$$\begin{aligned}\mathrm{Logit}(\Pi_{200}) = \beta \times [1 + \mathrm{D30} + \mathrm{D01} + \mathrm{D02} + \mathrm{PCP} + \mathrm{X}(\mathrm{D30}, \mathrm{AET30}) \\ \times (1 + \mathrm{TMP} + \mathrm{CD0}) + \mathrm{P}(\mathrm{TMP}) + \mathrm{P}(\mathrm{RH}) \\ + \mathrm{P}(\mathrm{POP}) \times (1 + \mathrm{D30}) + \mathrm{X}(\mathrm{V}) + \mathrm{FRA}]\end{aligned}$$

where Π_{200} is the probability of a fire >200 ha occurring, Logit(Π_{200}) is the logarithm of the odds ratio $(\Pi_{200}/(1-\Pi_{200}))$, β is a vector of parameters estimated from the data, and X(•) and P(•) are matrices describing basis spline and polynomial transformations of the data. The interaction terms:

$$\mathrm{X}(\mathrm{D30}, \mathrm{AET30}) \cdot (1 + \mathrm{TMP} + \mathrm{CD0})$$

result in estimation of a set of constants and a set of coefficients on average monthly temperatures and cumulative moisture deficits that are associated with the distribution of vegetation types and patterns of fire regime response to climate variability.

Table 2 Predictor variables

Variable	Description	>200 ha[1]	>8,500 ha[2]
D30	30-year average cumulative Oct.–Sep. moisture deficit	√	
AET30	30-year average cumulative Oct.–Sep. actual evapotranspiration	√	
D02	Cumulative 0ct.–Sep. moisture deficit, 2 years previous	√	
D01	Cumulative 0ct.–Sep. moisture deficit, 1 year previous	√	
CD0	Current water-year cumulative moisture deficit, Oct. through current month	√	
PCP	2-month cumulative precipitation, through current month	√	
RH	Monthly average Relative Humidity	√	√
TMP	Monthly average surface air Temperature	√	
V[3]	Vegetation Fraction	√	
POP	Total population (2000)	√	
FRA[3]	Federal protection responsibility area as percent of total area	√	
USFS[3]	USFS protection responsibility area as percent of total area		√
Aspect[4]	Average north/south facing		√

[1] Predictors for logistic regression estimating probability of a fire exceeding 200 ha

[2] Predictors for logistic regression estimating probability total burned area exceeds 8,500 ha conditional on one fire having exceeded 200 ha

[3] Fractions are transformed using $\log((\text{fraction} + .002)/(1 - \text{fraction} + .002))$ to generate a continuous variable centered around zero

[4] The transformation $\cos(\text{pi}/2 + \text{aspect}^*\text{pi}/180)$ yields the north/south component of aspect

The interaction terms:

$$\mathrm{P(POP)} \cdot (1 + \mathrm{D30})$$

capture direct effects of local population on the probability of large fire occurrence, which vary in this specification with the average summer moisture deficit in any given location. These factors may be indicative of several effects, including ignitions, accessibility, suppression resources, and suppression strategies.

We also estimate the probability that one or more very large fires burning in excess of 8,500 ha in aggregate may occur, conditional on there being at least one fire exceeding 200 ha:

$$\mathrm{Logit}(\Pi_{8500|200}) = \beta \times [1 + \mathrm{RH} + \mathrm{Aspect} + \mathrm{USFS}]$$

This model says that whether or not a large fire becomes a very large fire or not depends on the relative humidity, the north/south facing, and whether the fire is on Forest Service land or not. The latter variable might be related to management strategies, or it could simply be that so much of the forested area of the state, especially in less accessible locations, is managed by the Forest Service.

The probabilities estimated in this way can be summed to get an expected number of fires. For example, the number of wildfires >200 ha expected in California in a given year is just the sum of the probabilities Π_{200} for each of 12 months and 2,267 grid cells. The probabilities can also be used to simulate fire histories, drawing [0,1] randomly from binomial distributions with probabilities Π_{200} for each grid cell and month.

We also estimated generalized Pareto distributions (GPDs) for the logarithm of burned area for fires >200 ha and for fires >8,500 ha (for a discussion of methodology as it applies to wildfire and evidence that fire size regimes are consistent with heavy-tailed Pareto distributions, see Straus et al. 1989; Malamud et al. 1998; Ricotta et al. 1999; Cumming 2001; Song et al. 2001; Zhang et al. 2003; Schoenberg et al. 2003; Holmes et al. 2008). From these we estimated the expected burned area for a fire given that its area is greater than 200 ha and less than 8,500 ha, and the expected burned area for fires given that they are >8,500 ha. Expected burned area in any grid cell and month is thus:

$$\textbf{Expected Burned Area} = \Pi_{200} \times \widehat{A}\,|_{>200,<8500} + \Pi_{200} \times \Pi_{8500|200\cdot} \times \widehat{A}|_{>8500}$$

where the probabilities Π are as above, $\widehat{A}|_{>200,<8500}$ is the expected burned area less than 8,500 ha given that there is at least one fire greater than 200 ha, and $\widehat{A}|_{>8500}$ is the expected burned area given that at least 8,500 ha burned.

We use a two-step process like this because the empirical distribution of fire sizes in California appears to be non-stationary. Extremely large fires are governed by different processes than are more frequent large fires. As with the logistic regression results above, we can also draw randomly from the GPDs to simulate fire histories, generating a random burned area for each fire simulated with the binomial distributions.

3.2 Summary of scenarios

To summarize, we estimate 108 future scenarios, considering two emissions scenarios, three GCMs, two thresholds for defining urbanization, three scenarios for growth rates and the allocation of development, and three future time periods (Table 3).

4 Results and discussion

4.1 Model fit

The statistical significance of coefficients for the wildfire model specification was very stable across sub-samples, using cross-validation. The logistic regression for fires greater than 200 ha fit the observations well (Fig. 1), and the maximum probability of predicted fire occurrence was over 33%, which compares well with earlier fire models for climate change impact assessments in Westerling and Bryant (2008) and for seasonal forecasting in Preisler and Westerling (2007). The scale of interannual variation in expected fires aggregated statewide was comparable to that of observed fire. Forty-two percent of interannual variability in statewide large (>200 ha) wildfire occurrence was explained by the predicted probabilities, and the correlation between annual observed fire occurrence and predicted fire occurrence was highly significant (Spearman's ρ=0.73, p-value=0.0003). For monthly fire

Table 3 Summary of scenarios

Emissions	Model	Urban Threshold (households/km^2)	Growth Rate & Allocation	Period
SRES A2	CNRM CM3	147	LOW, LOW	2020
SRES B1	GFDL CM2.1	1,000	MID, MID	2050
	NCAR PCM1		HIH, HIH	2085

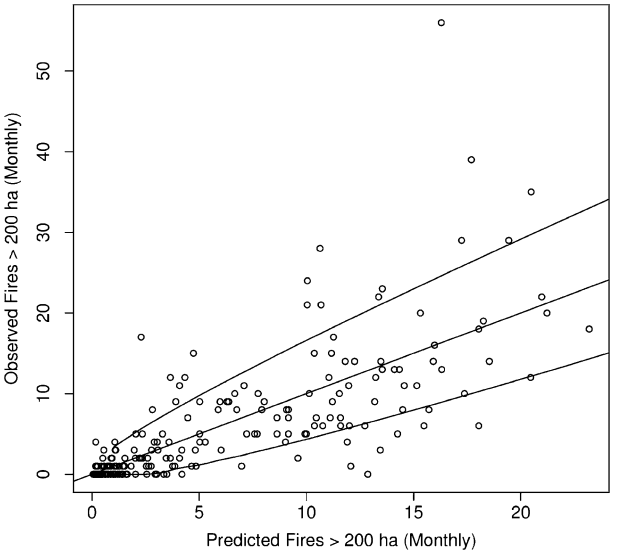

Fig. 1 Logistic regression model fit for fires>200 ha: Observed fire frequency (*vertical axis*) versus predicted probabilities (*horizontal axis*), binomial 95% confidence interval (*upper and lower lines*)

occurrence aggregated statewide, 58% of month-to-month variability was explained, and the correlation was also highly significant (Spearman's ρ=0.84, p-value=2e-16). The additional skill at the monthly time scale is due to the model fitting the seasonal cycle in the incidence of fires >200 ha, as well as the interannual variability.

Results for our estimation of the frequency of fires greater than 8,500 ha were also significant, but the skill was lower. This is likely due to both the small number of observed fires of this magnitude, and also it is likely that the size of these fires is highly sensitive to factors we are not able to consider here, such as the management strategy on individual fires, meteorological conditions on hourly to daily timescales during the fire, and landsurface characteristics at finer scales than those practical here (~12 km). Twenty percent of interannual variability in statewide very large (>8,500 ha) wildfire occurrence was explained by the predicted probabilities, and the correlation between annual observed and predicted very large fire occurrence was significant (Spearman's ρ=0.46, p-value= 0.04). Similarly, monthly predicted very large fire occurrence explained 23% of the variation in observed monthly values, and the correlation was highly significant (Spearman's ρ=0.46, p-value<7e-14).

While the Generalized Pareto Distribution fit the logarithm of monthly burned areas exceeding 200 ha and 8,500 ha very well (Fig. 2), the empirical fire size distributions still have a "fatter" right tail (i.e., higher probability of extremely large fires) than estimated by the modeled distributions, as indicated by the values to the far right in the Quantile plots sitting above the 1:1 ratio line (Fig. 2). This under-prediction of the extremes in fire size appears to be associated with two factors that are not captured in our modeling—a high degree of clustering in lightning-caused ignitions in some years, and high wind events (e.g. Santa Ana winds in coastal Southern California). Management factors may also play a role, such as the use of backfires, variation in the availability or effectiveness of suppression resources, and also a lack of consistency in reporting as fires both individual ignitions versus fire "complexes" resulting from multiple, coincident ignitions. The correlation between predicted and observed burned area was, however, highly significant (Spearman's ρ=0.82, p-value<2e-16).

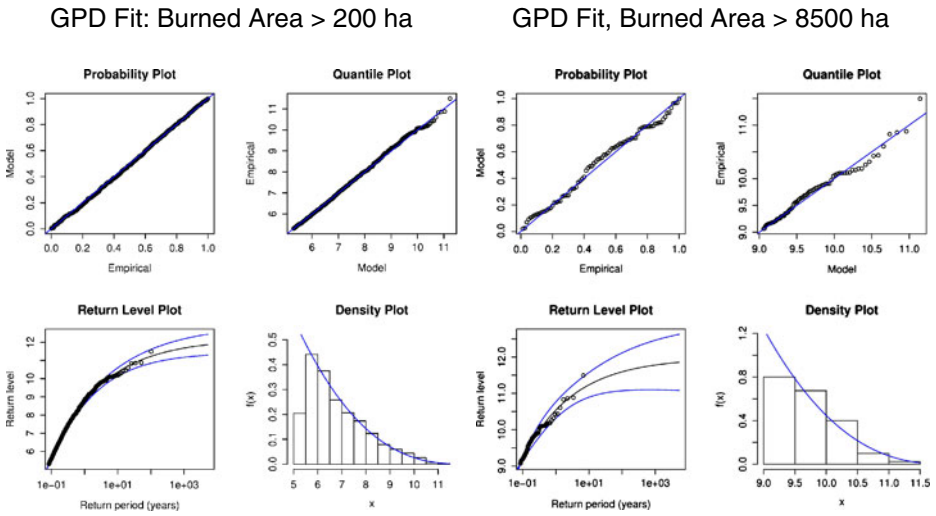

Fig. 2 Generalized Pareto Distributions fit to occurrence of burned area >200 ha (*left*) and burned area >8,500 ha (*right*). Distributions are fit to the logarithm of burned area and assume stationarity

Generalized Pareto Distributions can be fit with covariates such as climate and land surface characteristics, such that the parameters describing the distribution vary over time and space (see e.g., Holmes et al. 2008). We tested the full suite of predictor variables described in the preceding sections. While some of them were highly significant statistically, in practice including covariates had a trivial impact on our ability to predict year-to-year variations in burned area. Consequently, the results reported here use GPD fits assuming stationarity (i.e., that the fire size distribution does not change over time). Thus, the interannual variation in our predicted burned area is due entirely to variation in estimated probabilities for burned area to exceed the two specified thresholds (200 ha and 8,500 ha).

Together these four probabilistic models (logistic models of the probability of fire occurrence >200 ha and >8,500 ha, and Generalized Pareto Distributions for burned area >200 ha and >8,500 ha) can be used to estimate both the expected burned area at any given time and place in our modeling domain, and the associated variability implied by the four models around those estimates. Using random draws from binomial distributions with the probabilities predicted by logistic regressions, and random draws from Generalized Pareto Distributions, we simulated 1,000 fire histories over our gridded monthly model domain for 1980–1999, and aggregated them statewide by year (Fig. 3). Observed annual burned area was more variable than median simulated values, but within the range of variability across the simulations.

While for aggregate annual burned area for the state our combined models only explain about a quarter of interannual variability, the extremes in the residuals are accounted for by essentially two factors. Clusters of lightning-caused ignitions in a few outlying years in northern California account for a large part of the unexplained variability in large fire occurrence. Unexplained variability in burned area is in large part due to a combination of the effects of these lightning ignitions, and of Santa Ana-wind driven fire events in coastal southern California. Our climate-driven modeling is not able to predict the timing of lightning ignitions or Santa Ana winds. However, this range of variability is represented in

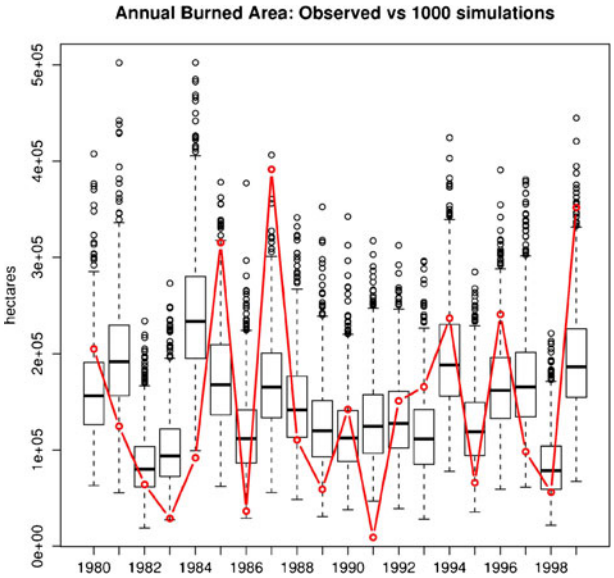

Fig. 3 Median (*horizontal lines*), interquartile range (*box*), extremes within 1.5 x interquartile range (*whiskers*) and extremes outside 1.5 x interquartile range are shown for annual burned area aggregated statewide for 1,000 simulations versus observed (*red line*) burned area for large fires in California. Predicted probabilities of large fires from logistic regressions, and Generalized Pareto distributions of fire size, were used to generate 1,000 simulations of burned area for each grid cell and month and then aggregated by year for the state for each simulation

the probabilities associated with fire occurrence and size in our models, and thus simulations using these probabilities do encompass the variability observed in burned area (Fig. 3).

4.2 Changes in California wildfire

Predicted large fire occurrence and total burned area increase over time for both emissions scenarios (Fig. 4).[2] Initial increases for burned area are relatively modest, with little difference between emissions scenarios—by 2020 the increases range from 6% to 23%, with median increases between 15% and 19%. By 2050 the spread in modeled outcomes widens, with predicted increases in burned area ranging from 7% to 41%, and median increases between 21% and 23%, but again differences due to emissions scenarios are relatively small compared to other factors. By 2085, the range of modeled outcomes is very large, with total burned area increasing anywhere from 12% to 74%. On average, the largest increases occur in 2085 for SRES A2 scenarios, with a median statewide increase in burned area of 44%, and the biggest increases occurring for the warmer, drier GFDL CM2.1 and CNRM CM3 model runs (range: 38%–74%, median 56%).

The SRES A2 scenarios in 2085 seem to be qualitatively different from either earlier periods or SRES B1 in 2085 (Fig. 4), implying that the most important policy implication of this study may be that moving to an emissions pathway more like that in SRES B1 (or lower) could be highly advantageous.

A robust result of this study is that forest burned area increases substantially—exceeding increases of 100% throughout much of the forested areas of Northern California—across all three of the GCMs analyzed here for the SRES A2 emissions scenario by 2085 (Fig. 5). To highlight the effects of potential increases in forest burned area, we analyzed a set of transects running from the edge of California's Central Valley near Merced northwest through the Sierra Foothills and Yosemite National Park to Mono Lake and Lee Vining on

[2] We show results for expected total area burned only, which are similar to predicted changes in large fire occurrence.

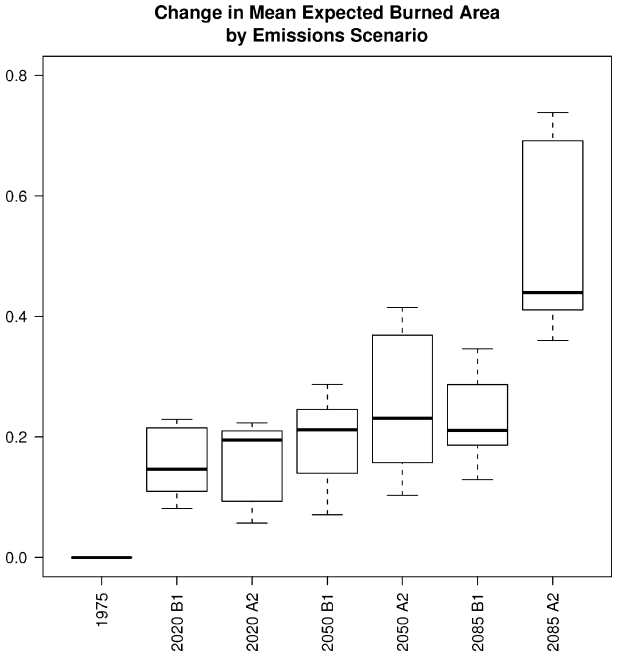

Fig. 4 Percentage change in expected burned area for large California fires from a 1961–1990 reference period for 108 scenarios, estimated for 30-year periods centered on the indicated dates, by emissions scenario. Bold horizontal lines indicate median scenario, boxes indicate middle 50% of values, *whiskers* indicate extremes

the eastern side of the Sierra Nevada range for a GFDL CM2.1 SRES A2 scenario with intermediate population growth and sprawl (MIDMID) and a high threshold for urbanization (Fig. 6). While increased temperatures and modest variations in precipitation generally resulted in similar increases in moisture deficit across the transects, the highest elevation sites were somewhat buffered by their greater available moisture. The largest

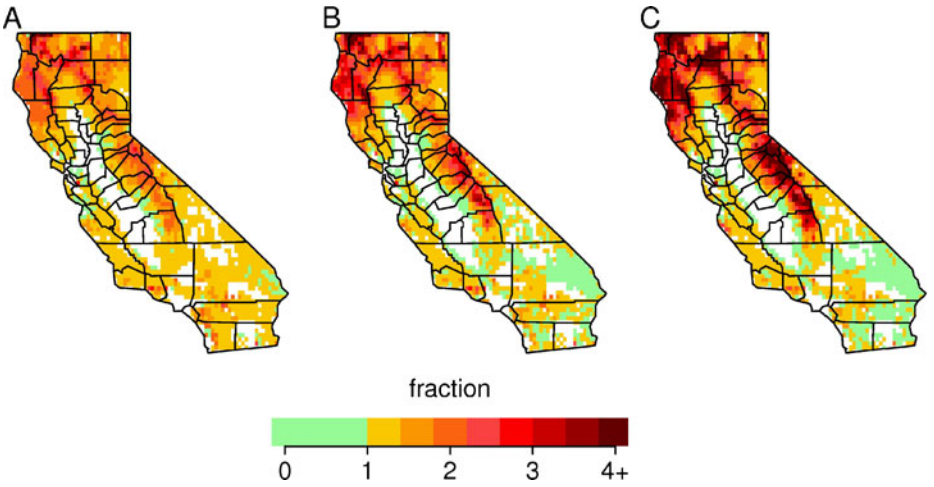

Fig. 5 2085 Predicted burned area as a multiple of reference period predicted burned area for three SRES A2 climate scenarios: **a** NCAR PCM1, **b** CNRM CM3, and **c** GFDL CM2.1, with high population growth, high sprawl, and a high threshold housing density for defining the limit to the wildland urban interface. The location of fire regimes is assumed to be fixed. A value of "1" indicates burned area is unchanged, while 4+ indicates that burned area is 400% or more of the reference period (i.e., a 300% increase)

increases in burned area tended to be mid-elevation sites on the west side of the Sierras. Much of the lower portion of these mid-elevation sites lies outside of federal reserves, and is comprised of private land holdings with very low-density development. In consequence, a significant portion of private households in this region of the state would be exposed to a substantially increased threat of wildfire under the SRES A2 emissions scenarios.

To highlight the effects of growth and sprawl on fire risks in the wildland urban interface in areas with a higher density of households, we analyzed model results for several SRES A2 scenarios on California's central coast, running from San Mateo County in the north through Santa Cruz to Monterey in the south, and east to San Benito and Santa Clara counties (Fig. 7). CNRM CM3 and GFDL CM2.1 model results were quite similar, though with higher burned area for GFDL CM2.1 (Fig. 7a&b). For both models, the largest increases were in Big Sur and the Ventana Wilderness, and in the redwood forests at the northern end of Santa Cruz county. High-growth, high-sprawl scenarios in this region tended to reduce burned area over a large region, as increased development reduced the vegetated area available to burn (Fig. 7c&d). Notably, results for rural northern Santa Cruz county were sensitive to the threshold set for determining when development becomes too dense for wildfires to occur (Fig. 7c&d).

The decrease in burned area in the southeastern deserts of California in Fig. 5 is the effect of greater drying across the three SRES A2 scenarios, which reduces fuel availability in these fuel-limited fire regimes.

5 Conclusion

We examine a range of future scenarios, considering multiple GCMs, emissions scenarios, and a range of growth and development scenarios. While the range of outcomes for these scenarios was large by the end of century, a majority of the scenarios indicated significant increases in large wildfire occurrence and burned area are likely to occur by mid-century. By 2085, substantial increases in large wildfire occurrence and burned area seem likely, particularly under the SRES A2 emissions scenarios, and particularly in forested areas of the state. This is mainly due to the effects of projected temperature increases on evapotranspiration in this scenario, compounded by reduced precipitation. The middle 50% of scenarios for SRES A2 in 2085 ranged from average statewide burned area increases of 41% to 69% compared to the reference period centered around 1975 (Fig. 4).

The spatial pattern of increased fire occurrence and burned area in the forests of Northern California was robust across a wide range of scenarios. Wildfire burned area increased dramatically throughout the mountain forest areas of Northern California across most of the various 2085 SRES A2 scenarios examined here. The SRES A2 scenarios by 2085 were qualitatively different from the B1 scenarios and the earlier period A2 scenarios in terms of the scale and spatial extent of increased fire occurrence and burned area. Given that we do, as a species, face choices regarding future emissions pathways, it would seem desirable to avoid persisting on a high greenhouse gas emissions pathway like A2.

Projected increases in burned area in the Sierra Nevada appear to be greatest for mid-elevation sites on the west side of the range. These are locations with significant areas outside of federally managed forest and park lands—and low-density development patterns—potentially exposing private landowners to substantially increased wildfire threats. To the extent that future low-density development in this region is vulnerable to

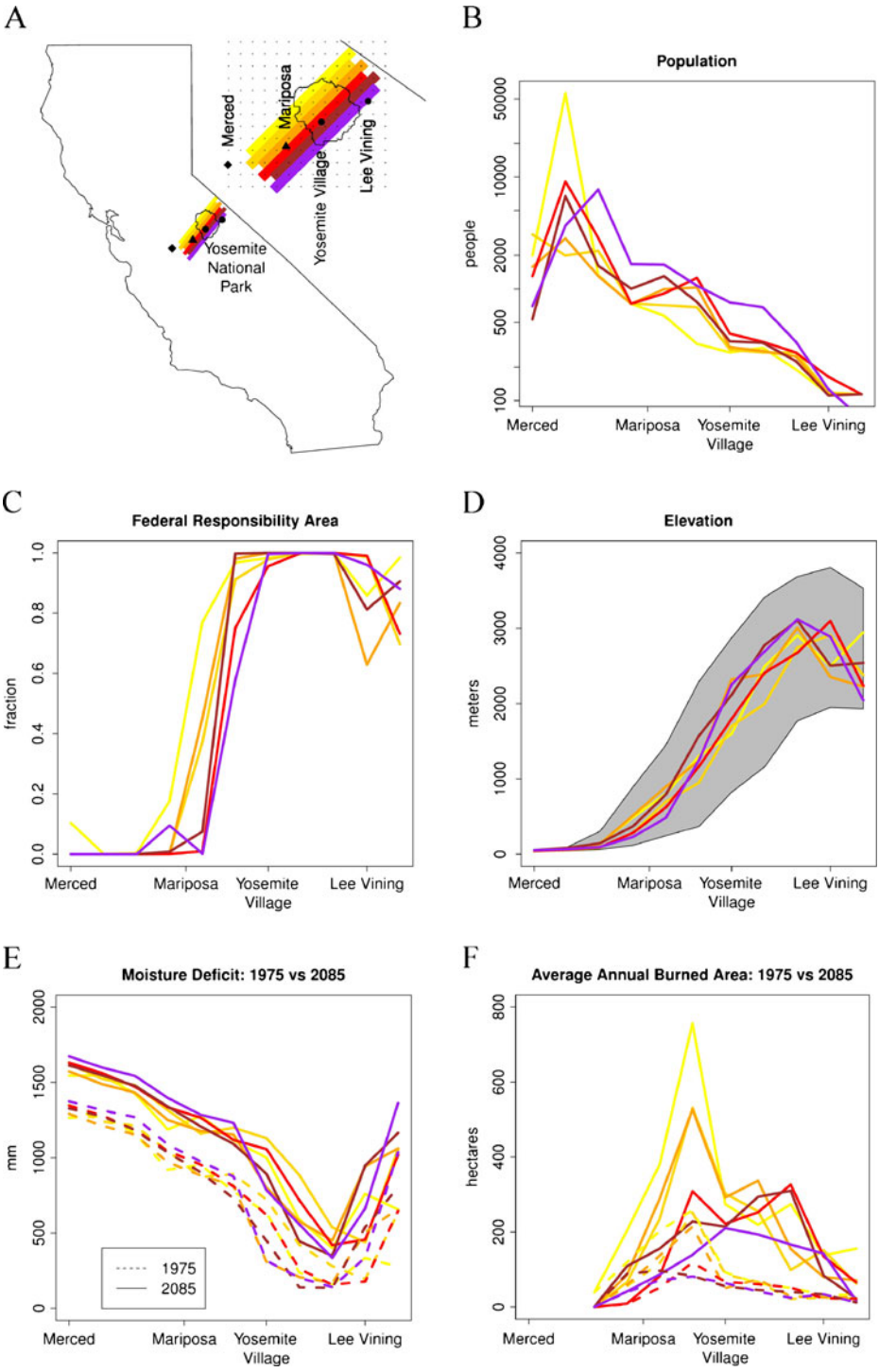
A
Merced
Mariposa
Yosemite Village
Lee Vining
Yosemite National Park
B
Population
people
100
500
2000
10000
50000
Merced
Mariposa
Yosemite Village
Lee Vining
C
Federal Responsibility Area
fraction
0.0
0.2
0.4
0.6
0.8
1.0
Merced
Mariposa
Yosemite Village
Lee Vining
D
Elevation
meters
0
1000
2000
3000
4000
Merced
Mariposa
Yosemite Village
Lee Vining
E
Moisture Deficit: 1975 vs 2085
mm
0
500
1000
1500
2000
1975
2085
Merced
Mariposa
Yosemite Village
Lee Vining
F
Average Annual Burned Area: 1975 vs 2085
hectares
0
200
400
600
800
Merced
Mariposa
Yosemite Village
Lee Vining

◀ **Fig. 6** **a** Six transects through the Sierra Nevada at Yosemite National Park with four reference communities; Color-coded by transect: **b** Population (*log scale*); **c** Federal area as a fraction of total area; **d** Mean elevation, and range (*shaded*); **e** 30-year Mean Annual Deficit and (**f**) Predicted Average Annual Burned Area

losses from fire, continued growth could increase the state's economic vulnerability to increased wildfire due to climate change.

Forest areas in coastal California also faced increased risk of wildfires under the warmer CNRM CM3 and GFDL CM2.1 SRES A2 scenarios, including iconic coastal redwoods and the Ventana wilderness area in central California. In contrast to communities in the Sierra foothills, continued sprawling growth around more densely settled communities in coastal California could actually reduce fire risks in some areas while increasing them in others. These results are sensitive to model assumptions that define the demarcation between areas where increased development is threatened by wildfire, and areas where urbanization has increased to the point where wildfires can no longer occur. This highlights an important area for further research.

The results presented here reflect a set of illustrative models and their underlying assumptions that together result in a cascading series of cumulative uncertainties, such that results for any one time and location cannot be considered a reliable prediction, even contingent on the scenario represented. While aggregating results over time and space and comparing outcomes against a common reference period estimated with the same methods and data sets can reduce the impact of some types of systematic error, these measures are not foolproof. Nonlinear effects of errors, or qualitative systematic changes over time that are not captured by our models, can lead to significant errors in future projections that are

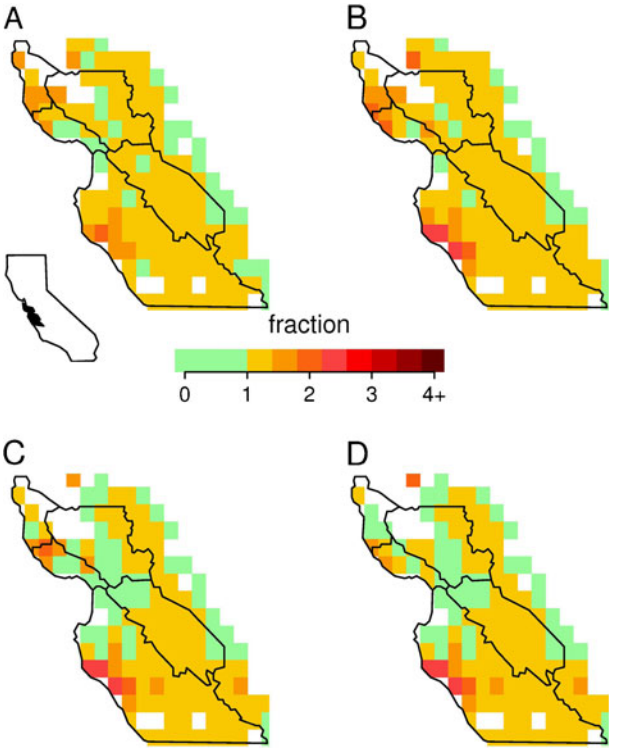

Fig. 7 Projected wildfire burned area around Monterey Bay communities for four scenarios **a** CNRM CM3 SRES A2, low growth and sprawl, high threshold for defining urbanized areas (1,000 households/km^2); **b** GFDL CM2.1 SRES A2, low growth and sprawl, high threshold for defining urbanized areas; **c** GFDL CM2.1 SRES A2, high growth and sprawl, low threshold for defining urbanized areas (147 households/km^2); (D) GFDL CM2.1 SRES A2, high growth and sprawl, high threshold for defining urbanized areas

not encompassed by the range of uncertainty represented in our results. That is, the results are conditional not only on the storylines of the SRES A2 and B1 scenarios and choice of global climate models, but also on the specifications of the statistical models of fire activity that we have estimated from historic data. To the extent that these data reflect processes that will no longer operate in the future because of qualitative changes to the systems we are modeling, our results will be in error.

Our results project the current managed fire regimes of California onto future scenarios for climate and for population and development footprint. We do not consider hypothetical effects of future changes in management strategies, technology, or resources that might be adopted with the intent of mitigating or adapting to the effects of climate and development on wildfire. Our models' implicit assumptions that such management effects are fixed may prove untenable under some future scenarios. Explicitly including management factors that can vary over the long term might significantly affect the outcomes modeled here in a systematic fashion. Such an exercise is left to a future study.

While we do not model metrics of fire severity (e.g., percent of vegetation consumed, ecological impact of burning) here, we expect that fire severity may be correlated with increases in fire occurrence and spatial extent in some ecosystems, particularly in some mountain forest areas of the state. It seems likely that outcomes such as those described here would have important implications for ecosystem services such as carbon sequestration in California forests, air pollution and public health, forest products and recreation industries, and the quality and timing of runoff from precipitation and snowmelt. All of these merit intensive further study.

References

Balling RC, Meyer GA, Wells SG (1992) Relation of surface climate and burned area in yellowstone national park. Agric For Meteorol 60:285–293

Brillinger DR, Preisler HK, Benoit JW (2003) Risk assessment: a forest fire example. In Science and Statistics, Institute of Mathematical Statistics Lecture Notes. Monograph Series

Cayan D, Tyree M et al (2009) Climate Change scenarios and sea level rise estimates for the California 2008 Climate Change Scenarios Assessment, Public Interest Energy Research, California Energy Commision, Sacramento, CA

Cumming SG (2001) A parametric model of the fire-size distribution. Can J For Res 31:1297–1303

Gesch DB, Larson KS (1996) Techniques for development of global 1-kilometer digital elevation models. In Pecora Thirteen, Human Interactions with the Environment—Perspectives from Space. Sioux Falls, South Dakota, August 20–22, 1996

Hamlet AF, Lettenmaier DP (2005) Production of temporally consistent gridded precipitation and temperature fields for the continental U.S. J Hydrometeorol 6(3):330–336

Hansen MC, DeFries RS, Townshend JRG, Sohlberg R (2000) Global land cover classification at 1 km spatial resolution using a classification tree approach. Int J Remote Sens 21:1331–1364

Heyerdahl EK, Brubaker LB, Agee JK (2001) Factors controlling spatial variation in historical fire regimes: a multiscale example from the interior West, USA. Ecology 82(3):660–678

Hidalgo HG, Dettinger MD, Cayan DR (2008) Downscaling with constructed analogues: Daily precipitation and temperature fields over the United States. CEC Report CEC-500-2007-123. January 2008

Holmes TP, Hugget RJ, Westerling AL (2008) Statistical analysis of large wildfires. Chapter 4 of economics of forest disturbance: Wildfires, storms, and pests, Series: Forestry Sciences, Vol. 79. In Holmes TP, Prestemon JP, Abt KL (Eds), XIV, p 422. Springer. ISBN: 978-1-4020-4369-7

Kipfmueller KF, Swetnam TW (2000) Fire-climate interactions in the Selway-Bitterroot wilderness area. USDA Forest Service Proceedings RMRS-P-15-vol-5

Le Quéré C, Raupach MR, Canadell JG, Marland G (2009) Trends in the sources and sinks of carbon dioxide. Nat Geosci 2:831–836

Liang X, Lettenmaier DP, Wood EF, Burges SJ (1994) A simple hydrologically based model of land surface water and energy fluxes for general circulation models. J Geophys Res 99(D7):14,415–14,428
Malamud BD, Morein G, Turcotte DL (1998) Forest fires: an example of self-organized critical behavior. Science 281:1840–1842
Maurer EP, Hidalgo HG (2008) Utility of daily vs. monthly large-scale climate data: an intercomparison of two statistical downscaling methods. Hydrology and Earth System Science 12:551–563
Maurer EP, Wood AW, Adam JC, Lettenmaier DP, Nijssen B (2002) A long-term hydrologically-based data set of land surface fluxes and states for the conterminous United States. J Climate 15:3237–3251
Mitchell KE et al (2004) The multi-institution North American Land Data Assimilation System (NLDAS): Utilizing multiple GCIP products and partners in a continental distributed hydrological modeling system. J Geophys Res 109:D07S90. doi:10.1029/2003JD003823
Monteith JL (1965) Evaporation and the environment. Symp Soc Expl Biol 19:205–234
Penman HL (1948) Natural evaporation from open-water, bare soil, and grass. Proc R Soc Lond A193 (1032):120–146
Preisler HK, Westerling AL (2007) Statistical model for forecasting monthly large wildfire events in the Western United States. J Appl Meteorol Climatol 46(7):1020–1030. doi:10.1175/JAM2513.1
Preisler HK, Westerling AL, Gebert KM, Munoz-Arriola F, Holmes T (2011) Spatially explicit forecasts of large wildland fire probability and suppression costs for California. International Journal of Wildland Fire 20:508–517
Preisler HK, Brillinger DR, Burgan RE, Benoit JW (2004) Probability based models for estimating wildfire risk. Int J Wildland Fire 13:133–142
Ricotta C, Avena G, Marchetti M (1999) The flaming sandpile: self-organized criticality and wildfires. Ecol Model 119:73–77
Schlobohm P, Brain J (2002) Gaining an understanding of the national fire danger rating system. National Wildfire Coordinating Group Publication: NFES # 2665. www.nwcg.gov
Schoenberg FP, Peng R, Woods J (2003) On the distribution of wildfire sizes. Environmetrics 14:583–592
Song W, Weicheng F, Binghong W, Jianjun Z (2001) Self-organized criticality of forest fire in China. Ecol Model 145:61–68
Stephenson NL (1998) Actual evapotranspiration and deficit: Biologically meaningful correlates of vegetation distribution across spatial scales. J Biogeog 25:855–870
Strauss D, Bednar L, Mees R (1989) Do one percent of the forest fires cause ninety-nine percent of the damage? Forest Sci 35:319–328
Swetnam TW, Betancourt JL (1998) Mesoscale disturbance and ecological response to decadal climatic variability in the American Southwest. J Clim 11:3128–3147
Theobald D (2005) Landscape patterns of exurban growth in the USA from 1980 to 2020. Ecol Soc 10(1):32
U.S. EPA (2008) Preliminary steps towards integrating climate and land use (ICLUS): The Development of Land-Use Scenarios Consistent with Climate Change Emissions Storylines (External Review Draft). U. S. Environmental Protection Agency, Washington, D.C. EPA/600/R-08/076A
Veblen TT, Kitzberger T, Donnegan J (2000) Climatic and human influences on fire regimes in ponderosa pine forests in the Colorado Front Range. Ecol Appl 10:1178–1195
Verdin KL, Greenlee SK (1996) Development of continental scale digital elevation models and extraction of hydrographic features. In: Proceedings, Third International Conference/Workshop on Integrating GIS and Environmental Modeling, Santa Fe, New Mexico, January 21–26, 1996. National Center for Geographic Information and Analysis, Santa Barbara, California
Westerling AL (2009) "Wildfires." Chapter 8 in Climate Change Science and Policy. Schneider, Mastrandrea, Rosencranz and Kuntz-Duriseti (Eds), Island Press"Washington DC, USA
Westerling AL, Bryant BP (2008) Climate change and wildfire in California. Clim Chang 87:s231–249. doi:10.1007/s10584-007-9363-z
Westerling AL, Gershunov A, Cayan DR, Barnett TP (2002) Long lead statistical forecasts of Western U.S. Wildfire area burned. Int J Wildland Fire 11(3,4):257–266. doi:10.1071/WF02009
Westerling AL, Brown TJ, Gershunov A, Cayan DR, Dettinger MD (2003) Climate and wildfire in the Western United States. Bull Am Meteorol Soc 84(5):595–604
Westerling AL, Hidalgo HG, Cayan DR, Swetnam TW (2006) Warming and earlier spring increases Western U.S. forest wildfire activity. Science 313:940–943. doi:10.1126/science.1128834, Online supplement
Zhang Y-H, Wooster MJ, Tutubalina O, Perry GLW (2003) Monthly burned area and forest fire carbon emission estimates for the Russian Federation from SPOT VGT. Remote Sens Environ 87:1–15